

OPEN ACCESS

EDITED BY
Sergiy M. Korogod,
Medicine and Rehabilitation
"Neuro-Universe", Ukraine

REVIEWED BY
Shanchun Su,
Duke University, United States
Emir Malovic,
University of Illinois Chicago, United States

*CORRESPONDENCE
Chaokun Li

☑ lichaokun@hotmail.com
Linlin Shan
☑ shanlinlin@xxmu.edu.cn

[†]These authors have contributed equally to this work

RECEIVED 11 August 2025 ACCEPTED 13 October 2025 PUBLISHED 28 October 2025

CITATION

Yue R-z, Guo X, Li W, Li C and Shan L (2025) HDAC7 knockout mitigates astrocyte reactivity and neuroinflammation via the IRF3/cGAS/STING signaling pathway. *Front. Cell. Neurosci.* 19:1683595. doi: 10.3389/fncel.2025.1683595

COPYRIGHT

© 2025 Yue, Guo, Li, Li and Shan. This is an open-access article distributed under the terms of the Creative Commons Attribution License (CC BY). The use, distribution or reproduction in other forums is permitted, provided the original author(s) and the copyright owner(s) are credited and that the original publication in this journal is cited, in accordance with accepted academic practice. No use, distribution or reproduction is permitted which does not comply with these terms.

HDAC7 knockout mitigates astrocyte reactivity and neuroinflammation via the IRF3/cGAS/STING signaling pathway

Rui-zhu Yue^{1†}, Xing Guo^{1†}, Wenqiang Li², Chaokun Li^{3*} and Linlin Shan^{3*}

¹College of Biological Sciences, China Agricultural University, Beijing, China, ²Henan Key Laboratory of Biological Psychiatry, The Second Affiliated Hospital of Xinxiang Medical University, Xinxiang, China, ³Department of Biochemistry and Molecular Biology, School of Basic Medical Sciences, Henan Medical University, Xinxiang, China

Introduction: Astrocytes are parenchymal cells widely distributed throughout the brain. Beyond their essential functions in healthy tissue, astrocytes exhibit an evolutionarily conserved response to all forms of brain injury, termed astrocytic reactivity. Nevertheless, conceptual understanding of what astrocytic reactivity encompasses and its functional roles remains incomplete and occasionally contentious. Lipopolysaccharide (LPS) is widely used to induce neuroinflammation. In the current study, Histone deacetylase 7 (HDAC7) has been shown to ameliorate LPS-induced neuroinflammation and mitigate astrocytic reactivity.

Methods: We overexpressed HDAC7 using viral vectors and generated primary astrocytes from Hdac7^{flox}/flox mice to achieve astrocyte-specific HDAC7 knockout. Subsequently, we assessed astrocytic reactivity and detected the expression of the Interferon regulatory factor 3 (IRF3)/cyclic GMP-AMP synthase (cGAS)/stimulator of interferon genes (STING) pathway.

Results: HDAC7 has been implicated in inflammatory regulation, but its role in astrocyte reactivity and the underlying mechanisms remain unclear. Here, we demonstrate that HDAC7 deficiency attenuates LPS-induced astrogliosis by suppressing the cGAS/STING signaling axis. LPS stimulation induced robust upregulation of glial fibrillary acidic protein (GFAP), complement component 3 (C3), and pro-inflammatory cytokines (TNF-α, IL-6) in WT astrocytes, which was significantly blunted in HDAC7 knockout astrocytes. Conversely, lentiviral overexpression of HDAC7 in WT astrocytes exacerbated IRF3/cGAS/STING pathway activation, as validated by Western blot analysis showing upregulated cGAS, STING and IRF3 expression. Pharmacological activation of the STING pathway in astrocytes restored pro-inflammatory cytokine expression and reactive marker levels, indicating pathway dependence.

Discussion: Our results delineate a novel HDAC7/IRF3/cGAS/STING signaling axis that governs astrocyte reactivity. This discovery provides a crucial cellular neurophysiological mechanism by which astrocytes integrate inflammatory signals and subsequently modulate the central nervous system

microenvironment. Targeting HDAC7, therefore, represents a therapeutic strategy to mitigate neuroinflammation by specifically correcting this aberrant cell-physiological state of astrocytes, ultimately preserving neural circuit function.

KEYWORDS

HDAC7, astrocyte, inflammation, LPS, IRF3, cGAS, STING, C3

1 Introduction

As the predominant glial subtype in the central nervous system (CNS), astrocytes are crucial for providing trophic and metabolic support to neurons, regulate synaptogenesis and neuroinflammatory responses, and contribute to blood-brain barrier (BBB) formation (Xiong et al., 2022). Reactive astrocytes are a state of astrocytes in the CNS that undergo morphological, physiological, and functional changes in response to injury or disease stimuli. They play a complex and dual role in pathological conditions. Specifically, when astrocytes differentiate into the A1 phenotype, reactive astrocytes become overactivated and release large amounts of pro-inflammatory cytokines (Liddelow et al., 2017). Excessive pro-inflammatory cytokines can further exacerbate the inflammatory response, leading to BBB, neuronal apoptosis, and neurological dysfunction. This process promotes the progression of neurodegenerative diseases, as excessive inflammation accelerates the death of nerve cells (Escartin et al., 2021; Hinkle et al., 2019; Liang et al., 2023).

This mechanism ensures immune quiescence during homeostasis and activates pro-inflammatory signaling in response to pathological stimulation. Under chronic neuroinflammation or infection, astrocytes adopt a neurotoxic A1 phenotype (Fang et al., 2022), marked by upregulation of complement proteins, pro-inflammatory cytokines (IL-6, TNF-α), and chemokines (CXCL10). This reactive astrogliosis can be induced by ATP/P2X7mediated Ca^{2+} signaling or microglial IL-1 α , TNF- α , and C1q. A1 astrocytes contribute to disease pathology via mechanisms such as oxidative stress in stroke (Sun et al., 2025; Wang et al., 2024), Excitatory amino acid transporter 2 (EAAT2) dysfunction in Amyotrophic Lateral Sclerosis (ALS) (Rosenblum et al., 2017), D-serine-mediated N-Methyl-D-aspartic acid (NMDA) potentiation in chronic pain (Sethuraman et al., 2009), C3driven synapse loss in Alzheimer's Disease (AD) (Wen et al., 2024), and neurotoxin release in HIV-associated neurocognitive disorders (HAND) (Lun et al., 2023). In contrast, A2 astrocytes

Abbreviations: AS, astrocyte; ATP, adenosine 5'-triphosphate; C3, complement C3; C1Q, complement component 1q; cGAS, Cyclic GMP-AMP synthase; COX-2, Cyclooxygenase-2; FKBP5, FK506-binding protein 5; GFAP, Glial fibrillary acidic protein; GFP, green fluorescent protein; GBP2, guanylate binding protein 2; H2–D1, Histocompatibility 2 class I antigen D 1; H2-T23, histocompatibility 2, T region locus 2 3; HDAC7, histone deacetylase 7; HSBP1, heat shock protein beta-1; IFN-γ, interferon-gamma; IL-1α, interleukin-1 alpha; IL-1β, interleukin-1 beta; IL-6, interleukin-6; INOS, inducible nitric oxide synthase; IRF3, interferon regulatory factor 3; Lcn2, lipocalin-2; LPS, lipopolysaccharide; NMDA, N-methyl-D-aspartic acid; PSMB8, proteasome subunit beta type 8; P2X7, purinergic receptor P2X 7; Serpina3n, serine peptidase inhibitor clade A member 3 n; STING, stimulator of interferon genes; TNF-α, tumor necrosis factor α; VIM, vimentin.

exert neuroprotective roles through Brain-derived neurotrophic factor/Glial-cell-line-derived neurotrophic factor (BDNF/GDNF) secretion and Aquaporin-4 (AQP4) -mediated edema regulation (Liddelow et al., 2017).

Class IIa histone deacetylases (HDACs 4, 5, 7, 9) modulate inflammation through epigenetic gene regulation and deacetylation of non-histone substrates in cancer (Shakespear et al., 2011). We investigated HDAC inhibition, which confers anti-inflammatory properties, in models of colitis and inflammation-induced tumorigenesis. The treatment demonstrated significant efficacy in suppressing both inflammation and tumor development (Glauben et al., 2009). HDAC7 overexpressed in astrocyte and was shown to promote nuclear factor kappa-light-chain-enhancer of activated B (NF-κB) activation and upregulate pro-inflammatory genes in LPS-induced mice (Ye et al., 2022). The IRF3/cGAS/STING pathway activates antiviral inflammation through type-I interferon (IFN-I) and NF-κB signaling (Balka et al., 2020). Recent studies implicate the cGAS-STING pathway in neuroinflammation (Paul et al., 2021), where cytosolic DNA sensing triggers Cyclic GMP-AMP (cGAMP) synthesis, STING activation, and IFN-I induction—observed in Aβ-mediated microglial activation in AD (Govindarajulu et al., 2023), antiviral responses in viral encephalitis (Losarwar et al., 2025), and STING knockout suppressing astrocyte proliferation (Zhang et al., 2020). Microglial STING activation contributes to neuroinflammation and neurodegeneration in α-synucleinopathies, including Parkinson's disease (PD) (Hinkle et al., 2022). The emergence of reactive astrocytes occurs concomitantly with neuroinflammation.

To date, no studies have demonstrated the involvement of HDACs in the IRF3/cGAS/STING system-induced inflammatory and reactive states of astrocytes. While our previous work established that LPS upregulates HDAC7 in astrocytes to drive pro-inflammatory responses via NF-κB activation, the precise mechanism by which LPS signaling promotes the polarization of astrocytes toward the detrimental A1 reactive state remains unknown. Here, we investigate whether the IRF3/cGAS/STING pathway serves as the critical link connecting LPS-induced HDAC7 upregulation to A1 astrocyte polarization.

2 Materials and methods

2.1 Animals

Hdac7^{flox/flox} mice were obtained from GenPharmatech. Adult C57BL/6 mice were purchased from Changzhou Cavens Laboratory Animal Co., Ltd (Changzhou, China).

 $Hdac7^{flox/flox}$ mice (4 months of age) were individually housed in ventilated cages (IVC; 4 mice per cage) under controlled temperature (22 \pm 1 °C) with a standardized 12 h/12 h light/dark cycle. Food (standard rodent chow) and water were provided *ad libitum*. All animal procedures were conducted in compliance with the National Institutes of Health Guide for the Care and Use of Laboratory Animals and were carried out under a protocol approved by the Institutional Animal Care and Use Committee (IACUC) of Xinxiang Medical University.

2.2 Primary astrocyte culture

Newborn Hdac7flox/flox mice (postnatal day 1-3) were selected, as cortical astrocytes are abundant and viable at this stage. Cortices were dissected under sterile conditions in a laminar flow hood. Meninges and hippocampi were carefully removed. Cortical tissues were transferred into dissociation solution (30 mL HBSS+330 μL HEPES+1.5 mL 10% Glucose) for enzymatic dissociation. An equal volume of 0.25% trypsin was added for 20 min digestion at 37 °C, terminated by adding 2 mL fetal bovine serum (FBS). The dissociated cell suspension was seeded onto poly-D-lysine (PDL)coated culture plates and maintained for 7 days in culture medium (90% DMEM high-glucose+10% FBS+1% penicillin/streptomycin). After 7 days, cells were placed on an orbital shaker (37 °C, 1,000 rpm for 12 h). The supernatant containing microglia and oligodendrocyte precursors was discarded. Adherent astrocytes were trypsinized and re-seeded onto new 6-well culture plates at a density of 5 \times 10⁶ cells/mL. Upon full adhesion, the cells were treated with 250 ng/mL LPS for 48 h before being harvested.

2.3 PCR

Genomic DNA extraction was performed using the Beyotime Mouse Genomic DNA Extraction Kit (D7283S). Freshly prepared digestion buffer (96 µL DNA Extraction Solution+4 µL Enzyme Mix per sample) was used to digest 0.2-1 cm tail tips, hair follicles with roots, or 10 μL saliva in 100 μL buffer (55 °C for 15 min \rightarrow 95 °C for 5 min). Reactions were terminated with 100 μL Stop Solution, with samples stored at -20 °C/4 °C. For PCR amplification, 20 µL reaction mixtures were prepared on ice containing: 7.4 µL dd H2O, 1 µL template DNA (2–20 ng/μL), 1.6 μL primer mix (Hdac7^{flox/flox} Forward: 5'-TCAGGAAGCCAGTACACCAGAA CTG-3'; Reverse: 5'-GGAAAGAGCTTGTGGGACGTCAC-3' Wild type: 247 bp, Mutant: 352 bp), and 10 μL Easy-LoadTM PCR Master Mix. After centrifugation, thermal cycling proceeded as: 95 °C 5 min (1 cycle); 10 cycles of [95 °C 20 sec \rightarrow 60 °C 20 sec (Δ -0.5 $^{\circ}$ C/cycle) \rightarrow 72 $^{\circ}$ C 50 sec]; 26 cycles of (95 $^{\circ}$ C 20 sec \rightarrow 55 $^{\circ}$ C 20 sec \rightarrow 72 $^{\circ}$ C 50 sec); final extension at 72 $^{\circ}$ C 5 min with temporary 4 °C hold. PCR products were directly analyzed by agarose gel electrophoresis. Critical precautions included: using sterile equipment, wearing gloves to prevent contamination, preparing digestion buffer fresh, and aliquoting samples for longterm storage to avoid freeze-thaw cycles (The results show in the Supplementary material).

2.4 Western blot

Primary astrocytes were lysed using RIPA buffer supplemented with protease and phosphatase inhibitors and subsequently harvested by cell scraping. The resulting lysates were sonicated on ice for 5 min, followed by centrifugation at 12,000 \times g for 20 min at 4 °C to collect the supernatant. Protein concentration was determined with a BCA assay kit (Beyotime, Cat# P0009). Protein samples were denatured in loading buffer at 95 °C for 10 min and electrophoresed on 10% or 12.5% SDS-polyacrylamide gels at 100 V for approximately 90 min. Subsequently, proteins were transferred onto nitrocellulose (NC) membranes (Thermo Fisher Scientific, Cat# 26616) at 256 mA for 30 min (proteins < 30 kDa) or 120 min (proteins 30-180 kDa). The membranes were blocked with 5% non-fat milk in TBST for 1 h at room temperature, incubated with primary antibodies (see Table 1) overnight at 4 °C, and then washed three times (10 min each) with TBST. Thereafter, membranes were probed with HRPconjugated secondary antibodies for 1 h at room temperature, followed by three additional washes with TBS. Protein bands were visualized using an enhanced chemiluminescence (ECL) detection system.

2.5 Realtime PCR

Total RNA was extracted from cultured cells with prechilled TRIzol $^{\mathrm{TM}}$ Reagent (Invitrogen, Cat# 15596026) according to the manufacturer's instructions. Briefly, after removing the culture medium, cells were directly lysed in TRIzol. RNA was precipitated through sequential phase separation using chloroform, followed by isopropanol precipitation and washing with 75% ethanol. The RNA pellet was collected by centrifugation at 12,000 \times g for 15 min at 4 °C. RNA concentration and purity were measured using a NanoDrop 2000 spectrophotometer (Thermo Fisher Scientific), and samples with A260/A280 ratios between 1.8 and 2.0 were used for subsequent experiments. First-strand cDNA was synthesized from total RNA using the PrimeScriptTM RT Master Mix (Takara Bio, Cat# RR047A). The process included two steps: (1) genomic DNA removal with gDNA Eraser at 25 °C for 5 min, and (2) reverse transcription at 37 °C for 15 min, followed by enzyme inactivation at 85 °C for 5 sec and cooling to 4 °C. Realtime PCR was performed on a Bio-Rad CFX96 Real-Time PCR System using 2× Real Star Fast SYBR qPCR Mix (Gene Star, Cat# A301-10). Each 10 μL reaction contained 5 µL of qPCR mix, 0.8 µL each of forward and reverse primers (10 µM), 2 µL of cDNA template, and $2.2~\mu L$ of nuclease-free water. The thermal cycling conditions were as follows: initial denaturation at 95 °C for 30 sec; 40 cycles of 95 °C for 5 sec and 60 °C for 30 sec; and melt curve analysis from 60 to 95 °C with incremental heating at 0.5 °C/sec. Threshold cycle (Cq) values were determined using Bio-Rad CFX MaestroTM software. Relative mRNA expression levels were calculated via the $2^{-\Delta \Delta Ct}$ method, with glyceraldehyde-3-phosphate dehydrogenase (GAPDH) serving as the endogenous reference gene. Primer sequences can are listed in Table 2.

TABLE 1 Primers used for realtime PCR.

| Genes | Forward (5' to 3') | Reverse (5' to 3') | |
|-----------|-------------------------------|-------------------------------|--|
| GAPDH | TGTGAACGGATTTG GCCGTA | ACTGTGCCGTTGAAT TTGCC | |
| HDAC7 | GAACTCTTGAGCCCT TGGACA | GGTGTGCTGCTACT ACTGGG | |
| C3 | AAGCATCAACACACC CAACA | CTTGAGCTCCATTCGT GACA | |
| C1Q | AAAGGCAATCCAGGCA ATATCA | TGGTTCTGGTATGGA CTCTCC | |
| COX-2 | GTCTGGTGCCTGGT CTGATGATG | TCTGATACTGGAACTGCT GGTTGAA | |
| FKBP5 | GGACTGGACAGTGC CAATGAGA | CGTTGTGCTCCTT CGCCTTC | |
| GFAP | AGAAAGGTTGAATC GCTGGA | CGGCGATAG TCGTTA | |
| GBP2 | CCTGGTTCTGCTTGAC ACTGAG | TGCTGGTTGATGGTTC CTATGC | |
| H2-D1 | GGCTCCACAGATAC CTGAAGAAC | CAAGAGGCACCACC ACAGATG | |
| H2-T23 | CTCCTCCATCCACTG TCTCCAA | ACCTATGTGTCTCCTC CTCTTCAT | |
| HSBP1 | ATCCCCTGAGGGCAC ACTTA | GGAATGGTGATCTCCG CTGAC | |
| IFN-γ | CGGCACAGTCATT GAAAGCC | TGCATCCTTTTTCG CCTTGC | |
| IL-1α | CGCTTGAGTCGGC AAAGAAAT | CTTCCCGTTGCTT GACGTTG | |
| IL-1β | GCAACTGTTCCTG AACTCAACT | ATCTTTTGGGGTC CGTCAACT | |
| IL-6 | TAGTCCTTCCTACCCCAA TTTCC | TTGGTCCTTAGCCACT CCTTC | |
| iNOS | CCCTTCCGAAGTTTCTGG CAGCAGC | GGCTGTCAGAGCCTCGTGG CTTTGG | |
| Lcn2 | TGGCCCTGAGTGTC ATGTG | CTCTTGTAGCTCATAGAT GGTGC | |
| PSMB8 | CACCGCATTCCTGAGG TCCTT | GGAGTCCACAGCCAC GATGA | |
| Serpina3n | ATTTGTCCCAATGTCT GCGAA | TGGCTATCTTGGCTATAA AGGGG | |
| TNF-α | CCCTCACACTCAGATCA TCTTCT | GCTACGACGTGGG CTACAG | |
| VIM | CGTCCACACGCACCTACAG | GGGGGATGAGGAAT AGAGGCT | |

2.6 Immunofluorescence

Cells were fixed with 4% paraformaldehyde for 15–20 min to preserve cellular morphology. Permeabilization was carried out with 0.3% Triton X-100 (P0096, Beyotime) for 30 min to facilitate antibody access. Following this, blocking was performed with 5% BSA at room temperature for 1 h to minimize nonspecific binding. Subsequently, primary antibodies, diluted to their optimal working concentrations, were applied and incubated overnight at 4 °C to allow specific antigen binding. The next day, samples underwent three 5 min PBS washes to remove unbound primary antibodies.

TABLE 2 Primary antibodies used in this study.

| Antibodies | Applications | Source | Catelogy |
|------------|--------------|---------------|-------------|
| β-actin | WB: 1:2,000 | Proteintech | Cat#66009 |
| cGAS | WB: 1:1,000 | Proteintech | Cat#29958 |
| STING | WB: 1:1,000 | CST | Cat#13647S |
| IRF3 | WB: 1:1,000 | Proteintech | Cat#66670 |
| INOS | WB: 1:1,000 | CST | Cat#13120S |
| COX-2 | WB: 1:1,000 | Abcam | Cat#ab15191 |
| IL-6 | WB: 1:1,000 | CST | Cat#12912S |
| IL-1β | WB: 1:1,000 | Proteintech | Cat#16806 |
| GFAP | WB: 1:1,000 | CST | Cat#3670S |
| HDAC7 | WB: 1:1,000 | Sigma-Aldrich | Cat# H2662 |

Fluorescently conjugated secondary antibodies were incubated for 1 h at 37 °C protected from light. After three additional 5 min PBS washes to remove excess secondary antibodies, nuclei were counterstained with DAPI for 5 min. Mounted specimens were imaged using fluorescence microscopy.

2.7 Flow cytometry

Prior to the initiation of the procedure, all necessary reagents were prepared, including 1X PBS, 4% formaldehyde, 100% methanol, and 0.5% BSA in PBS (stored at 4 °C). For fixation, adherent cells or tissues were dissociated into single-cell suspensions and centrifuged at 150-300 g for 5 min to pellet the cells. The cell pellet was resuspended in approximately 100 μL of 4% formaldehyde per 1×10^6 cells and mixed thoroughly to dissociate aggregates and prevent cell clumping. Fixation was performed at room temperature (20-25 °C) for 15 min. After fixation, cells were washed 2-3 times with excess 1X PBS via centrifugation - care being taken to avoid excessive g-forces to prevent cell rupture - and finally resuspended in 0.5-1 mL of 1X PBS for immediate use or stored overnight at 4 °C. For permeabilization, fixed cells were gently resuspended, and prechilled 100% methanol was added dropwise to achieve a final concentration of 90%, followed by incubation on ice for at least 10 min. For immunostaining, an appropriate number of cells were aliquoted into 1 mL microcentrifuge tubes, washed 2-3 times with 1X PBS under gentle centrifugation, and incubated with 100 µL of primary antibody solution for 1 h at room temperature with occasional mixing. Cells were then washed again and incubated with 100 µL of secondary antibody solution for 1 h at room temperature protected from light. After a final wash, cells were resuspended in 200-500 µL of 1X PBS. Processed samples were analyzed using a flow cytometer. The purity of astrocytes was assessed by flow cytometry, and the representative gating strategy and quantification are presented in Supplementary Figure 2.

2.8 ELISA

Quantification of interleukin-6 (IL-6) and interleukin-1 beta (IL-1 β) in lysates of primary astrocytes was performed using

specific ELISA kits (MEIMIAN, #MM-0163M1 and #MM-0040M1, respectively) in strict adherence to the manufacturer's protocol. The assay procedure involved the addition of 50 μL of standards or samples to the antibody-precoated wells, followed by a 30-min incubation at 37 °C. The wells were then aspirated and washed three times with wash buffer. Subsequently, 100 μL of horseradish peroxidase (HRP)-conjugated detection antibody was added to each well, and the plate was incubated for a further 30 min at 37 °C. After a second wash cycle, color development was initiated by sequential addition of 50 μL of substrate solutions A and B, with a 15-min incubation at 37 °C in the dark. The enzymatic reaction was stopped by adding 50 μL of stop solution per well. Absorbance was measured immediately at 450 nm, and sample cytokine concentrations were determined by interpolation from a standard curve calibrated with recombinant proteins.

2.9 Statistical analysis

Statistical analyses were performed with Graphpad Prism 10 (LaJolla, CA, USA). Unpaired Student's t-test was employed to identify difference between the two groups. One-way or two-way analysis of variance (ANOVA) followed by Tukey's multiple comparisons test was employed to identify differences among three or more groups as indicated in the figure legends. The statistical significance levels were set at p < 0.05 (*), p < 0.01 (***), p < 0.001 (***), with a confidence interval of 95%. All data were expressed as mean \pm SD.

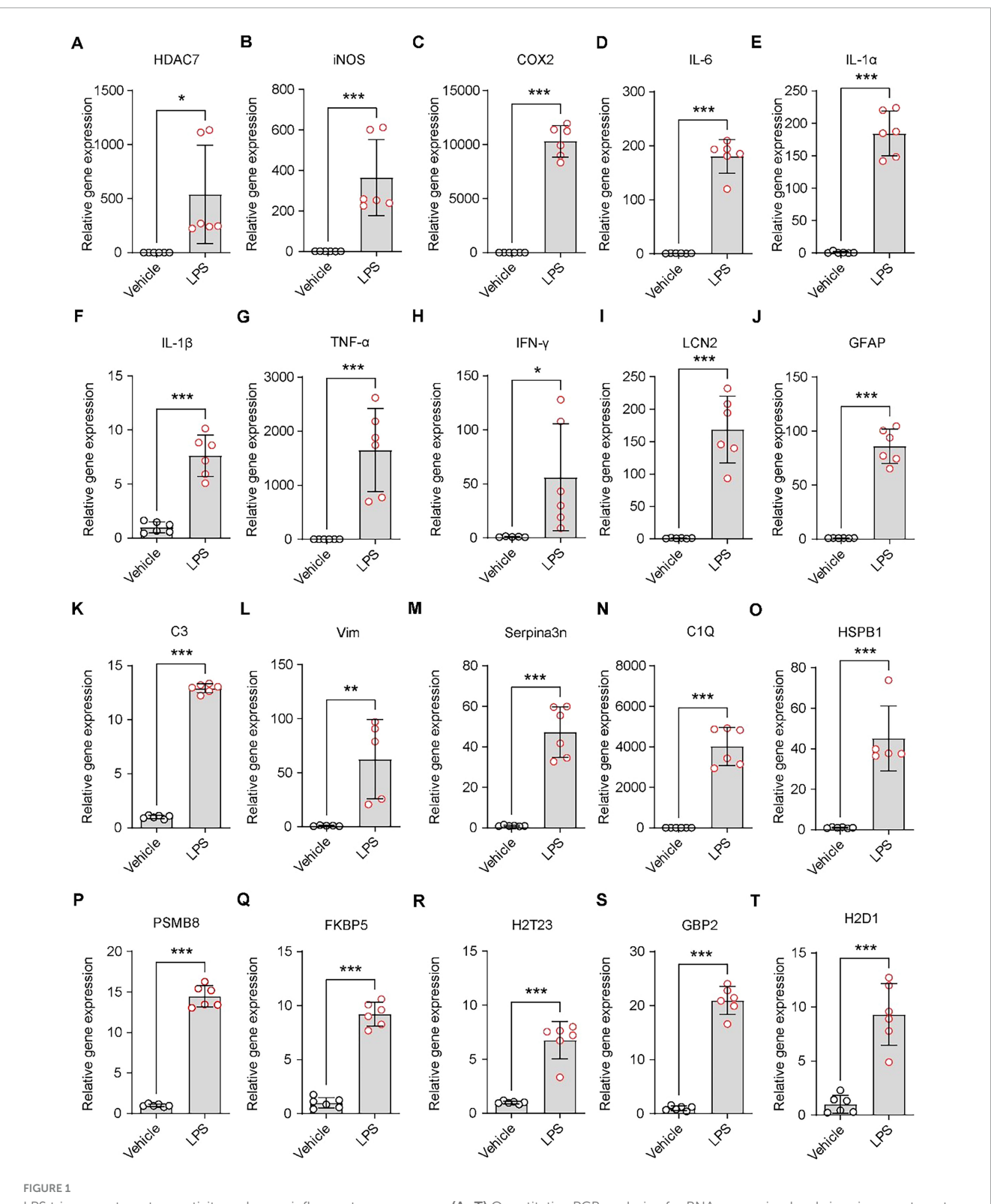
3 Results

3.1 LPS triggers astrocyte reactivity and neuroinflammatory responses

Following treatment of primary astrocytes with 250 ng/mL LPS for 48 h, we detected HDAC7 expression to validate our previous findings (Ye et al., 2022), confirming that LPS induces significant upregulation of HDAC7 (Figure 1A). iNOS, an enzyme increased during inflammation, primarily catalyzes nitric oxide (NO) production (Hibbs et al., 1988; Moncada et al., 1991). NO exhibits cytotoxicity by damaging DNA, proteins, and cell membranes (Xia et al., 2010). Concurrently, NO upregulates other pro-inflammatory factors (e.g., IL-1β, TNF-α), establishing a pro-inflammatory positive feedback loop. LPS markedly increased iNOS expression (Figure 1B), accompanied by elevated IL-1β (Figure 1F) and TNFα expression (Figure 1G). COX-2, a key enzyme in prostaglandin synthesis (Kujubu et al., 1991), showed significant upregulation in astrocytes under sustained LPS stimulation (Figure 1C). A pronounced increase in IL-6 further indicated progressive enhancement of astrocytic inflammatory responses (Figure 1D). Peripheral administration of LPS is known to trigger a central inflammatory response and robustly stimulate IL-1α expression from astrocytes (Figure 1E). While inducing substantial elevations in inflammatory gene (iNOS, COX-2, IL-1β, TNF-α), LPS also significantly upregulated IFN-γ expression (Figure 1H). LCN2, initially identified in neutrophils and widely expressed in various cells (epithelial, immune, neuronal), participates in inflammatory and immune responses (Kjeldsen et al., 1994). It demonstrated marked upregulation following stimulation by inflammatory cytokines (IL-1β, TNF-α, IFN-γ) (Figure 1I). Elevated LCN2 further amplified TNF-α and IL-6 release. GFAP, a specific astrocytic marker critical for maintaining cellular structure, function, and CNS homeostasis (Bignami et al., 1972), showed significant overexpression (Figure 1J) in activated "reactive astrocytes," accompanied by cellular hypertrophy and increased processes. Astrocytic complement C3 expression, observed in various pathological conditions, was substantially increased by LPS (Figure 1K). Vimentin (Vim), a type III intermediate filament protein, is predominantly expressed in radial glia and immature astrocytes during CNS development, later replaced by GFAP in adults. In mature brain tissue, Vim persists in subependymal immature astrocytes and cerebellar Bergmann glia (Hockfield and McKay, 1985). LPS induced Vim upregulation in astrocytes (Figure 1L). Serpina3n, an acute-phase protein with anti-inflammatory effects in early cerebral ischemia by suppressing microglial overactivation (Zhang J. et al., 2021), exhibited sustained overexpression under LPS-induced model (Figure 1M), potentially promoting pro-inflammatory A1 astrocyte maintenance and impairing neural repair. Under neuroinflammatory conditions, inflammatory microglia secrete IL-1a, TNF, and C1q to induce astrocytic activation into neurotoxic states. Our study confirmed LPS-induced IL-1α and TNF upregulation, with concurrent C1Q elevation (Figure 1N), indicating significant neuroinflammation and A1 reactive astrocyte transformation. HSBP1, a reactive astrocyte marker, was upregulated by LPS (Figure 1O). LPSinduced PSMB8 overexpression (Figure 1P) triggered endoplasmic reticulum stress and excessive inflammatory cytokine release (IFN-y, IL-6). While astrocytes normally support myelination, LPS-induced A1 transformation led to FKBP5 overexpression (Figure 1Q), inhibiting remyelination. Classic A1 astrocyte markers H2-T23, GBP2, and H2-D1 all showed significant LPS-induced upregulation (Figures 1R-T).

3.2 Overexpression of HDAC7 activates IRF3/cGAS/STING and induces astrocyte activation and inflammatory responses

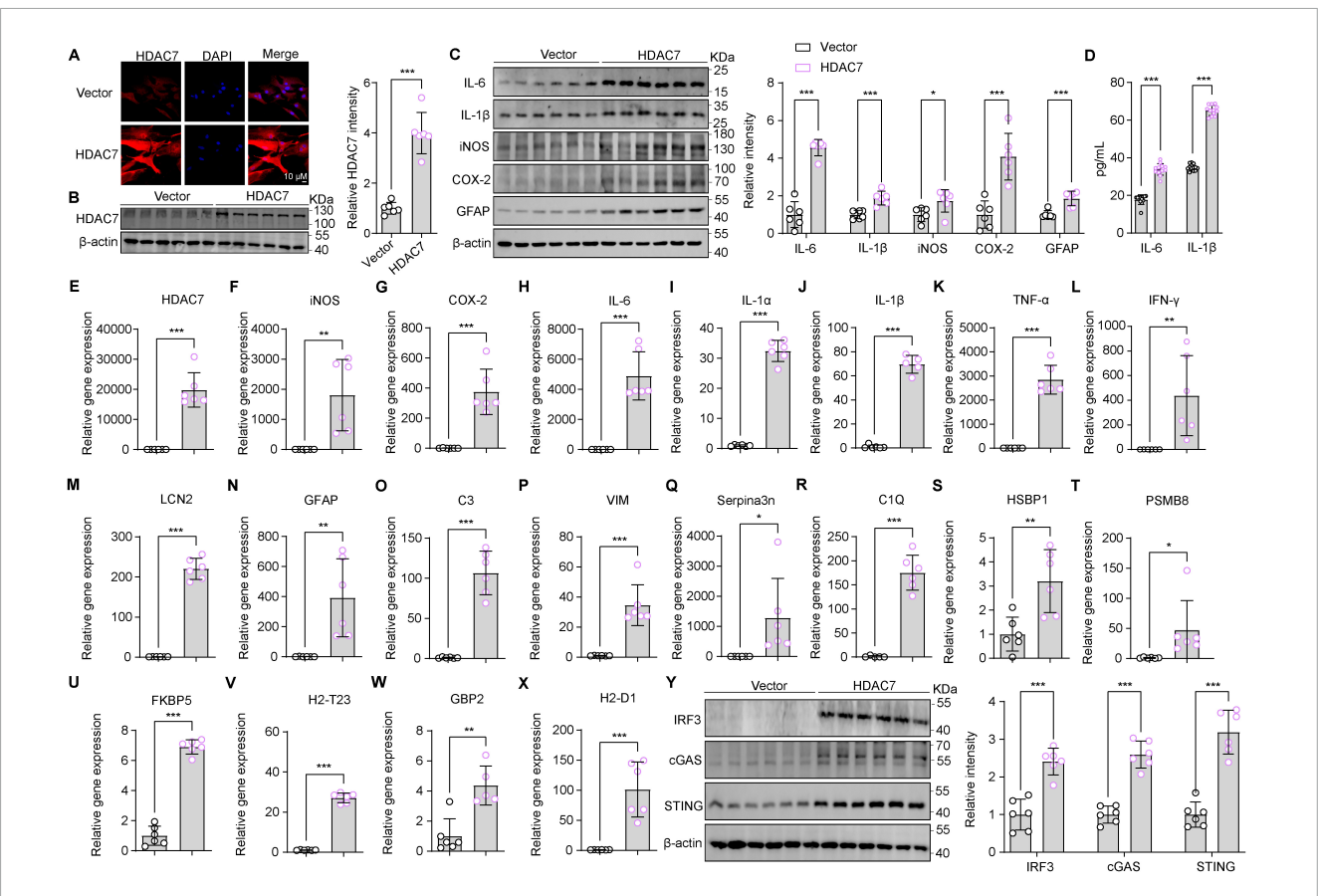
Building on our previous finding that LPS upregulates astrocytic HDAC7—which enhances IKKα/β acetylation, activates NF-κB, and drives neuroinflammation—we next questioned whether HDAC7 overexpression alone is sufficient to induce astrocyte activation (Ye et al., 2022). Next, we identified whether HDAC7 overexpression can induce astrocyte activation. Primary mouse astrocytes transduced with LV-GfaABC1D-HDAC7-GFP-WPRE showed substantial upregulation of HDAC7 at both the mRNA and protein levels (Figures 2A, B, E). This was accompanied by a pronounced increase in the expression of key proinflammatory mediators—iNOS, COX-2, IL-6, and IL-1β are highly increased in protein and mRNA (Figures 2C, F-H, J). Notably, the elevated levels of IL-6 and IL-1β were further confirmed by ELISA (Figure 2D), demonstrating a consistent and significant upregulation. Reactive astrocyte marker GFAP (Figure 2N), additional cytokines IL-1α, TNF-α and IFN-γ (Figures 2I, K, L) were also elevated. Notably, HDAC7 overexpression upregulated



LPS triggers astrocyte reactivity and neuroinflammatory responses. (A–T) Quantitative PCR analysis of mRNA expression levels in primary astrocytes treated with 250 ng/mL LPS. (A) HDAC7, (B) iNOS, (C) COX-2, (D) IL-6, (E) IL-1 α , (F) IL-1 α , (G) TNF- α , (H) IFN- γ , (I) LCN2, (J) GFAP (K) C3, (L) Vim, (M) Serpina3n, (N) C1Q, (O) HSBP1, (P) PSMB8, (Q) FKBP5, (R) H2-T23, (S) GBP2, and (T) H2-D1, n=5-6. Data are presented as mean \pm SD. Statistical significance was determined using unpaired t-test. ***p < 0.001, **p < 0.001, **p < 0.05.

both general (LCN2, GFAP) and A1-specific (C3, C1Q, GBP2) reactive astrocyte markers (Figures 2M–X), establishing HDAC7 as a key driver of A1 astrocyte transformation. Importantly,

HDAC7 overexpression in astrocytes also significantly activated components of the STING pathway, including IRF3, cGAS, and STING (Figure 2Y).



Overexpression of HDAC7 activates IRF3/cGAS/STING and induces astrocyte activation and inflammatory responses. (A) Representative immunostaining images of HDAC7 and DAPI in astrocyte (Scale Bar = $10 \mu m$). (B) Representative Western blot images for HDAC7 and β -actin, and the corresponding quantitative data, n = 6. (C) Representative Western blot images of IL-6, IL-1 β , iNOS, COX-2, GFAP and β -actin, with quantification of band intensities indicating the relative protein expression levels of IL-6, IL-1 β , iNOS, COX-2 and GFAP, n = 6. (D) IL-6 and IL-1 β concentrations were measured by ELISA, n = 12. (E-X) Quantitative PCR analysis of mRNA expression levels of various inflammatory and oxidative stress markers including (E) HDAC7, (F) iNOS, (G) COX-2, (H) IL-6, (I) IL-1 α , (J) IL-1 β , (K) TNF- α , (L) IFN- γ , (M) LCN2, (N) GFAP, (O) C3, (P) Vim, (Q) Serpina3n, (R) C1Q, (S) HSBP1, (T) PSMB8, (U) FKBP5, (V) H2-T23, (W) GBP2, and (X) H2-D1 in primary astrocyte infected with AAV-GfaABCD-GFP-WARE and AAV-GfaABCD-HDAC7-GFP-WARE, n = 5-6. (Y) Representative Western blot images showing the expression of IRF3, cGAS, STING, and β -actin, with quantification of band intensities indicating the relative expression levels of IRF3, cGAS, and STING, n = 6. Data are presented as mean \pm SD. Data are presented as mean \pm SD. Statistical significance was determined using unpaired t-test. ***p < 0.001, **p < 0.01, *p < 0.01, *p < 0.05.

3.3 HDAC7 deletion inhibits IRF3/cGAS/STING and ameliorates reactive astrogliosis and neuroinflammatory responses

Building upon our finding that HDAC7 upregulation drives astrocyte transformation into reactive A1 astrocytes, we generated Hdac7^{flox/flox} mice and isolated primary astrocytes from neonates. Cells were transduced with pLenti-EF1-P2A-puro-CMV-Cre-3xFLAG-WPRE to knockout HDAC7, assessing whether this attenuates LPS-induced inflammation and reactivity. Western blot analysis and immunofluorescence confirmed a significant reduction in HDAC7 expression following viral infection (Figures 3A, B, F). Additionally, we monitored key inflammatory markers, including cytokines (IL-6, IL-1β) and enzymes (iNOS, COX-2). HDAC7 knockout significantly attenuated the LPS-induced upregulation of these factors, as demonstrated by both western blot, Elisa and quantitative PCR analyses (Figures 3C, D, G–K). The reduced expression levels of IL-6 and IL-1β were

further validated by ELISA in primary astrocytes, confirming consistent suppression following HDAC7 knockout (Figure 3E). Finally, we examined the effect of HDAC7 knockout on reactive astrocytes and found it significantly downregulated both general (LCN2, GFAP) and A1-specific (C3, C1Q, GBP2) markers (Figures 3L–Y), confirming its inhibitory role in A1 astrocyte polarization. Additionally, HDAC7 knockout suppressed LPS-induced activation of the cGAS/STING pathway (Figure 3Z). Collectively, these results indicate that HDAC7 deficiency prevents astrocytes from transforming into A1 reactive astrocytes.

3.4 HDAC7 deletion mitigates STING pathway-driven reactive astrogliosis and neuroinflammatory responses

Building upon our finding that HDAC7 upregulation drives astrocyte transformation into reactive A1 astrocytes. Next, to assess whether HDAC knockout can attenuates LPS-induced

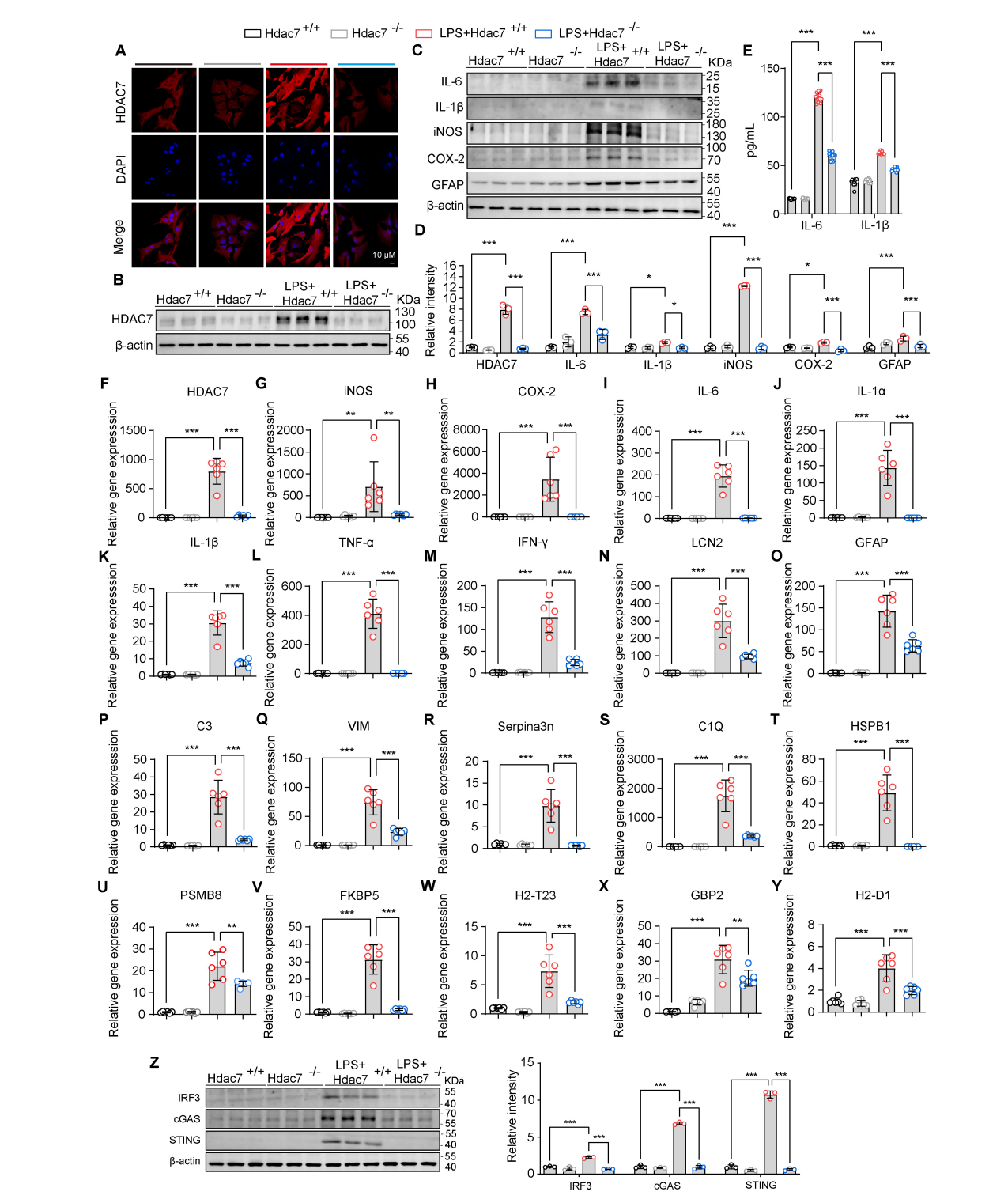


FIGURE 3
HDAC7 deletion inhibits IRF3/cGAS/STING and ameliorates reactive astrogliosis and neuroinflammatory responses. (A) Representative immunostaining images of HDAC7 and DAPI in astrocyte (Scale Bar = 10 μm). (B) Representative Western blot images of HDAC7 and β-actin, n = 3. (C) Representative Western blot images of IL-6, IL-1β, iNOS, COX-2, GFAP and β-actin, n = 3. (D) Quantification of HDAC7, IL-6, IL-1β, iNOS, COX-2, GFAP protein expression levels normalized to β-actin. (E) IL-6 and IL-1β concentrations were measured by ELISA, n = 12. (F-Y) Quantitative PCR analysis of mRNA expression levels of various inflammatory and reactive astrocyte markers including (F) HDAC7, (G) iNOS, (H) COX-2, (I) IL-6, (J) IL-1α, (K) IL-1β, (L) TNF-α, (M) IFN-γ, (N) LCN2, (O) GFAP, (P) C3, (Q) Vim, (R) Serpina3n, (S) C1Q, (T) HSBP1, (U) PSMB8, (V) FKBP5, (W) H2-T23, (X) GBP2, and (Y) H2-D1, n = 5 - 6. (Z) Representative Western blot images of IRF3, cGAS, STING, and β-actin, with quantification of band intensities indicating the relative expression levels of IRF3, cGAS, and STING. The primary astrocyte transfected with pLenti-EF1-P2A-puro-CMV-3xFLAG-WPRE (HDAC7^{+/+}) and pLenti-EF1-P2A-puro-CMV-3xFLAG-WPRE (HDAC7^{-/-}). And We treated primary astrocytes with 250 ng/mL LPS, n = 3. Data are presented as mean ± SD. Statistical significance was determined using one-way ANOVA with Tukey's post-hoc test. ***p < 0.001, **p < 0.01, **p < 0.05.

inflammation and reactivity, primary astrocyte derived from Hdac7flox/flox mice were transduced with G10 (a specific STING agonist). We investigated whether HDAC7 knockout could suppress astrocyte toxicity and reactive phenotypes. Initially, we assessed the expression levels of key inflammatory mediators at both protein and mRNA levels. The results showed significant reductions in IL-6, IL-1β, iNOS, and COX-2 (Figures 4B-D, F, U). Notably, the decreased expression of IL-6 and IL-1 β was further confirmed by ELISA, consistent with the preceding data (Figure 4V). We also detected the reactive astrocyte activation marker GFAP and found it was also significantly reduced (Figure 4J). We detected the expression of IRF3 and cGAS and found significant decreases (Figure 4U), indicating that HDAC7 knockout inhibits the IRF3/cGAS/STING pathway. Next, we detected HDAC7 mRNA expression and found a significant decrease, suggesting that activating the STING pathway to induce inflammatory factor release also stimulates HDAC7 overexpression (Figure 4A). We also detected other relevant inflammatory factors, such as IL-1α (Figure 4E), TNF-α (Figure 4G), and IFN-γ (Figure 4H), and found that these inflammatory factors also decreased significantly, indicating that HDAC7 knockout can reduce the increased release of inflammatory factors caused by STING pathway activation. Finally, we verified whether HDAC7 knockout could inhibit the activation of reactive astrocytes and the high expression of A1 astrocyte markers after STING pathway activation. We found that reactive astrocyte markers, including LCN2 (Figure 4I), HSBP1 (Figure 4O), Serpina3n (Figure 4M), VIM (Figure 4L), and GFAP (Figure 4J) were significantly decreased; while established A1 astrocyte markers such as C3 (Figure 4K), C1Q (Figure 4N), PSMB8 (Figure 4P), FKBP5 (Figure 4Q), H2-T23 (Figure 4R), GBP2 (Figure 4S), and H2-D1 (Figure 4T) also showed significant reductions.

4 Discussion

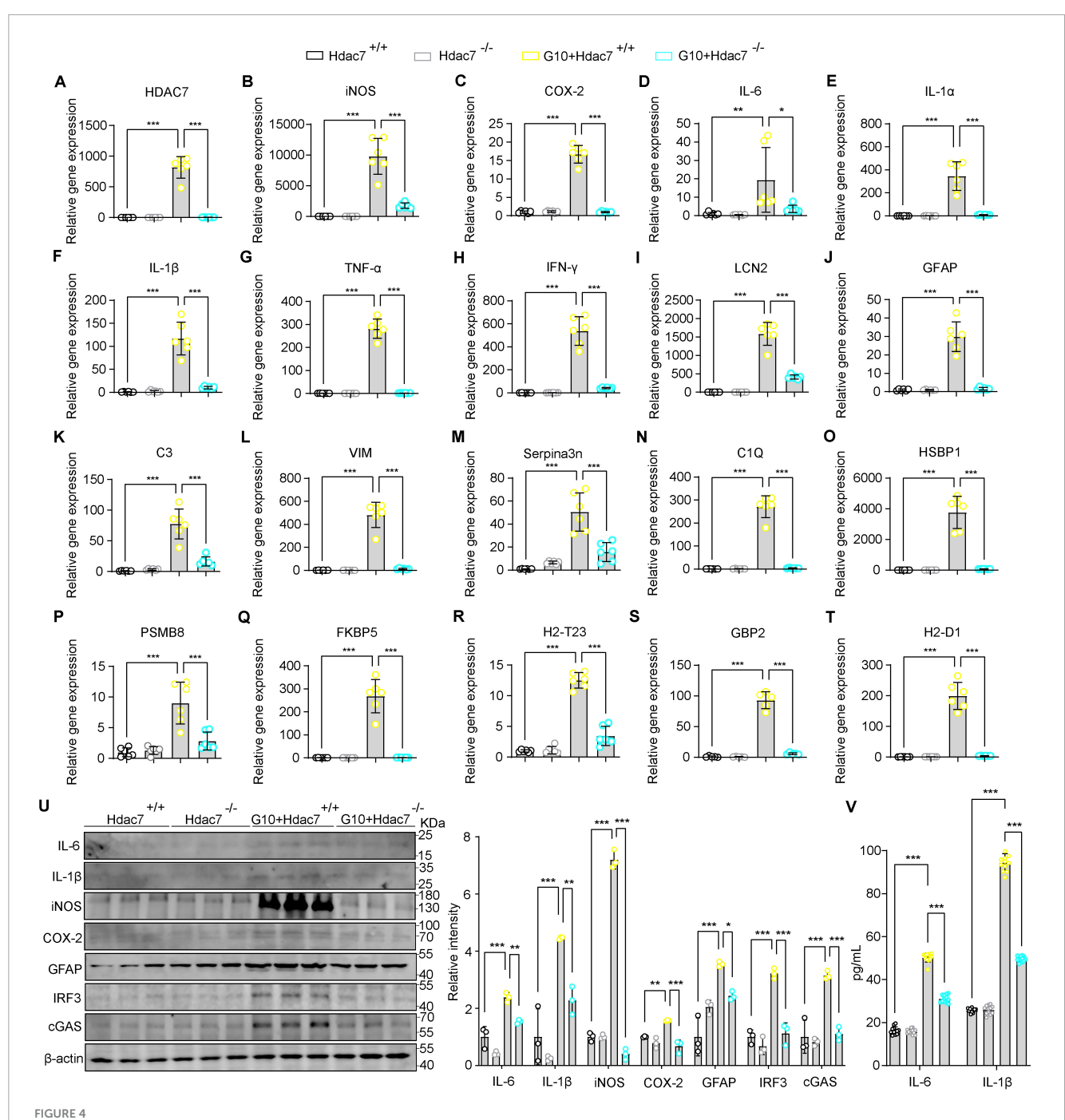
This study systematically reveals the critical regulatory role of HDAC7 in LPS-induced A1 astrocyte activation and neuroinflammation, and for the first time demonstrates that HDAC7 drives neurotoxic astrocyte polarization by activating the IRF3/cGAS/STING signaling pathway, as validated by genetic knockout models showing the significant inhibitory effect of HDAC7 deficiency on neuroinflammation.

Glial cells are key components of the central nervous system with diverse and complex functions. Under physiological conditions, astrocytes interact with neurons through the "tripartite synapse" structure, directly regulating synaptic transmission and plasticity. They are responsible for maintaining extracellular ion/transmitter homeostasis and providing neurotrophic support. Meanwhile, microglia, as resident immune cells, play a central role in immune surveillance (Hanslik et al., 2021; Segarra et al., 2019; Vecino et al., 2016). A1 astrocyte activation is a common feature in pathological processes such as neurodegenerative diseases and brain injury (Hinkle et al., 2019); their overactivation can exacerbate neuronal damage by releasing complement proteins, pro-inflammatory cytokines, and neurotoxins (Yun et al., 2018). Elucidating the intrinsic mechanisms regulating neurotoxic versus neuroprotective astrocyte phenotypes

remains a current research priority. Evidence indicates that the previously simplified A1: neurotoxic astrocyte and A2: neuroprotective astrocyte classification can be further subdivided into distinct subpopulations defined by proliferative capacity and differential gene expression profiles (Batiuk et al., 2020). Neuroprotective astrocytes act via compartmentalized cyclic adenosine monophosphate (cAMP) produced by soluble adenylyl cyclase. This regulation restrains microglial activation, leading to the suppression of downstream neurotoxic astrocyte induction (Cameron et al., 2024). Some studies also indicate that microglia play pivotal roles in the nervous system. Pharmacological or genetic approaches can induce robust adult neurogenesis (Dräger et al., 2022; Willis et al., 2020; Zhang Y. et al., 2021). Evidence further demonstrates that activated microglia release multiple inflammatory factors including IL-6, IL-1α, and TNF which drive astrocyte transformation into A1 astrocytes, thereby exacerbating severe neuroinflammatory responses in the nervous system (Liddelow et al., 2017). LPS-induced systemic inflammation leads to the generation of reactive astrocytes. The levels of inflammatory factors in astrocytes are significantly increased; it also exacerbates the activation of microglia, the disruption of the BBB, the infiltration of peripheral immune cells, neuronal dysfunction, and the depressive behaviors of mice (Guo et al., 2024). Under pathological conditions, factors such as neuroinflammation can activate microglia, which in turn drives the transformation of astrocytes into a neurotoxic A1-reactive phenotype. These reactive astrocytes release large amounts of pro-inflammatory factors, compromising BBB integrity and triggering neuronal apoptosis, thereby accelerating the progression of neurodegenerative diseases. In this process, molecules such as HDAC7 play a crucial role in glial cell activation and inflammatory responses by modulating key signaling pathways like IRF3/cGAS/STING, making them potential therapeutic targets for intervening in neuroinflammation and related diseases.

Therefore, the current discussions on A1 astrocytes remain inconclusive and are still a subject of debate. However, this study primarily focuses on elucidating the transformation mechanisms of normal astrocytes into A1-type astrocytes.

HDACs play a crucial role in modulating astrocyte function and neuroinflammation (Beurel, 2011; Manengu et al., 2024). In the context of neuroinflammation, HDACs modulate astrocyte activation, driving these cells toward a reactive phenotype marked by heightened generation of pro-inflammatory cytokines and chemokines (Wang et al., 2023). This astrocyte activation can exacerbate the inflammatory response and contribute to the compromise of the BBB (Kim et al., 2022). Targeting HDACs represents a potential therapeutic strategy to modulate astrocyte-mediated neuroinflammation and mitigate the associated neurodegenerative processes (Cai et al., 2022). Overexpression of Sirt1 reduces the reactivity of astrocytes, improves neurological dysfunction and improves neuron activity (Zhang et al., 2019, 2022). Additionally, HDACs may influence the crosstalk between astrocytes and other glial cells, such as microglia, further amplifying neuroinflammatory signaling (Villarreal et al., 2021). Our research found that LPS stimulation significantly upregulates HDAC7 expression in astrocytes, and HDAC7 overexpression further enhances the release of A1 markers and pro-inflammatory factors, suggesting HDAC7 is a key molecule linking PAMPs stimulation to the cytotoxic astrocyte phenotype.



HDAC7 deletion mitigates STING pathway-driven reactive astrogliosis and neuroinflammatory responses. (A–T) Quantitative PCR analysis of mRNA expression levels of various inflammatory and oxidative stress markers including (A) HDAC7, (B) iNOS, (C) COX-2, (D) IL-6, (E) IL-1 α , (F) IL-1 β , (G) TNF- α , (H) IFN- γ , (I) LCN2, (J) GFAP (K) C3, (L) Vim, (M) Serpina3n, (N) C1Q, (O) HSBP1, (P) PSMB8, (Q) FKBP5, (R) H2-T23, (S) GBP2, and (T) H2-D1. The primary astrocyte transfected with pLenti-EF1-P2A-puro-CMV-3xFLAG-WPRE (HDAC7^{+/+}) and pLenti-EF1-P2A-puro-CMV-Cre-3xFLAG-WPRE (HDAC7^{-/-}). And We treated primary astrocytes with 10 μ M G10 (as the agonist of sting), n = 5–6. (U) Representative Western blot images of IL-6, IL-1 β , iNOS, COX-2, GFAP, IRF3, cGAS, and β -actin, with quantification of band intensities indicating the relative expression levels, n = 3. (V) IL-6 and IL-1 β concentrations were measured by ELISA, n = 12. Data are presented as mean \pm SD. Statistical significance was determined using one-way ANOVA with Tukey's post-hoc test. ***p < 0.001, **p < 0.05.

Activation of the cGAS-STING axis orchestrates a multifaceted cellular program that encompasses senescence, autophagy, selective mRNA translation, and robust interferon-driven immunity (Wu et al., 2024). The cGAS/STING pathway is a central signaling axis for cytosolic DNA sensing. It is indispensable for mounting antiviral defenses, yet its dysregulation fuels autoimmune

pathology and drives neuroinflammatory cascades (Oduro et al., 2022). This study found that HDAC7 overexpression significantly activates the protein expression of IRF3, cGAS, and STING, whereas HDAC7 deficiency reduces LPS or G10-induced inflammatory responses by inhibiting this pathway. It is noteworthy that STING activation can feedback to upregulate

HDAC7 mRNA levels, suggesting a potential positive feedback regulatory loop between HDAC7 and the cGAS/STING pathway, which jointly sustains the chronicity of neuroinflammation. HDAC7 knockout mouse models constructed using CRISPR/Cas9 show that HDAC7 deficiency significantly inhibits LPS-induced astrocyte hypertrophy, GFAP expression, and upregulation of A1 markers, while concurrently reducing levels of pro-inflammatory factors such as IL-1 β and TNF- α in brain tissue.

Under neuroinflammatory stress, LCN2 is rapidly synthesized and secreted by activated microglia and reactive astrocytes, propagating a cytotoxic milieu that culminates in widespread neuronal apoptosis. We demonstrate that LCN2 secretion from reactive astrocytes is triggered by LPS as an inflammatory stressor. Studies indicate that inhibiting NF-KB activation downregulates astrocytic LCN2 even under inflammatory stress (Jung et al., 2023). Our findings show that suppressing HDAC7 overexpression in astrocytes ameliorates LCN2 elevation, concurrently validating our prior research that NF-KB pathway activation enhances inflammatory factor release effects attenuated by TMP195mediated inhibition of histone deacetylase function (Ye et al., 2022). Furthermore, this study establishes HDAC7 as a mediator of astrocyte transformation into A1-type reactive astrocytes. Mechanistically, this protective effect is closely associated with the inactivation of the IRF3/cGAS/STING pathway, indicating that HDAC7 may serve as a potential target for intervening in neuroinflammation-related diseases.

As research into the pathological mechanisms neurodegenerative diseases advances, the neuroregulatory roles of HDACs and their specific inhibitors in these disorders are becoming increasingly elucidate. However, the physiological functions of HDAC7 in the nervous system, particularly its regulatory mechanisms in the activation of A1-reactive astrocyte, remain poorly understood and require further investigation. Based on our in vitro experimental results, we propose a central hypothesis: the HDAC7/cGAS-STING signaling pathway identified in this study may represent a key molecular mechanism driving the sustained activation of neurotoxic A1-reactive astrocytes. This mechanism could potentially explain the core pathological feature observed in neurodegenerative diseases such as Alzheimer's disease namely, the persistent activation of astrocytes and exacerbated neuroinflammatory damage that are difficult to alleviate. Furthermore, future studies should focus on elucidating the regulatory patterns of this pathway in vivo using disease models, validating the synergistic neuroprotective effects of HDAC7specific inhibitors and cGAS-STING pathway interventions, and clarifying the crosstalk between this pathway and other neuroinflammatory signaling cascades (Ye et al., 2022, 2025).

In the cGAS-STING signaling pathway, the initiation stage begins with the sensing of cytosolic double-stranded DNA. When exogenous DNA, such as viral DNA, or endogenous DNA, such as mitochondrial DNA leakage caused by genomic instability, is present in the cytoplasm, cGAS binds to and is activated by these dsDNA molecules. Subsequently, activated cGAS catalyzes the synthesis of the cyclic dinucleotide second messenger 2'3'-cGAMP from ATP and GTP. During the signal transduction phase, STING located on the endoplasmic reticulum, inducing conformational changes and dimerization of STING. The activated STING protein then translocates from the endoplasmic reticulum to the perinuclear region via the Golgi apparatus (Newman et al., 2024;

West et al., 2015). Downstream STING activation involves the recruitment and activation of TBK1, leading to the phosphorylation and nuclear translocation of IRF3 and NF- κ B, where they drive the expression of type I interferons (IFN- α / β) and inflammatory cytokines to trigger a broad innate immune response (Jiao et al., 2023). Previous studies have shown that class IIa HDACs can significantly activate IRF3 (Lu et al., 2024). Inspired by this finding, we investigated whether HDAC7 might also activate the cGAS-STING signaling pathway. In our study, we found that knockout of HDAC7 suppressed the cGAS-STING signaling pathway, thereby preventing excessive inflammatory responses in astrocytes.

HDAC7, a member of Class IIa histone deacetylases, exerts context-dependent and often complex regulatory roles in inflammation across different tissues and cell types. Its functions extend beyond histone modification to include deacetylation of transcription factors and cytoplasmic proteins, thereby influencing key inflammatory signaling pathways. In immune cells such as macrophages, HDAC7 is generally recognized as a positive regulator of pro-inflammatory responses. It enhances NF-κB activation and significantly upregulates the expression of proinflammatory cytokines such as TNF-α, IL-6, and IL-1β. The mechanism primarily relies on direct interaction with TRAF6 and TAK1 in the TLR4 signaling pathway, amplifying downstream MAPK and NF-κB activation without altering chromatin accessibility. Studies have shown that HDAC7 expression is significantly increased in LPS-induced inflammation models, and targeted degradation of HDAC7 using PROTAC technology effectively suppresses the release of multiple inflammatory cytokines (Kadier et al., 2024). The role of HDAC7 in inflammatory regulation remains incompletely understood; however, our findings indicate that it promotes the activation of the cyclic cGAS-STING pathway and exacerbates neuroinflammation. HDAC7 is a key regulator in TLR signaling. Its enzymatic activity can be rapidly activated by various TLR agonists in a MyD88 adaptor-dependent manner. This protein plays a dual role in inflammation: it regulates glycolysis in macrophages induced by low-dose LPS in a deacetylase-independent manner, while through its enzymatic activity-particularly via deacetylation of PKM2 and subsequent promotion of HIF-1α-mediated transcription—it enhances the production of pro-inflammatory cytokines such as IL-1 β and CCL2. This functional divergence positions HDAC7 as a critical node linking inflammation and metabolic reprogramming, especially in low-grade chronic inflammation. Targeting HDAC7 enzymatic activity or its mediated protein interactions offers a potential new strategy for treating inflammation-related diseases (Ramnath et al., 2022). While current research has mainly focused on the strong pro-inflammatory role of HDAC7 in macrophages, studies also indicate that HDAC7 plays a significant pro-inflammatory role in LPS-induced inflammation by promoting the activation of astrocytes (Ye et al., 2022). Given its significant impact on inflammatory processes, HDAC7 has emerged as a potential therapeutic target in inflammatory and autoimmune diseases. Inhibition of HDAC7 has been shown to attenuate excessive immune activation in several experimental models, and our experiments further supplement its important role in ameliorating neuroinflammation, suggesting its utility in modulating inflammation-driven pathology.

Reactive astrogliosis, a hallmark of various neurological disorders, is characterized by the morphological and functional

transformation of astrocytes in response to pathological stimuli. Several biomarkers have been identified to delineate reactive astrocytes (Liddelow et al., 2017). Activation of the IRF3/cGAS/STING pathway in microglia and astrocytes promotes the release of pro-inflammatory cytokines, chemokines, and interferons, exacerbating neuroinflammation (Decout et al., 2021).

It is noteworthy that HDAC7, belonging to class IIa HDACs, possesses tissue-specific expression and regulates non-histone substrates; these properties may confer lower systemic toxicity compared to broad-spectrum HDAC inhibitors, providing a theoretical basis for developing central nervous system-selective anti-inflammatory drugs. Although this study clarified the mechanism of HDAC7 action in in vitro astrocyte models, its role within the complex in vivo neural microenvironment requires further validation. For instance, whether HDAC7 indirectly influences neuroinflammation by regulating microglia-astrocyte interactions or exerts differential functions at distinct disease stages such as acute injury vs. chronic degeneration, needs to be elucidated by in vivo experiments. Furthermore, the interaction of HDAC7 with other inflammatory pathways, such as the NLRP3 inflammasome (Yao et al., 2022), and its impact on astrocyte differentiation toward the neuroprotective A2 phenotype, also warrants in-depth investigation. The functional plasticity of astrocytes makes them a potential therapeutic target for neurological diseases. Future research needs to leverage singlecell sequencing and spatial transcriptomics to decipher their heterogeneity and develop dual regulatory strategies, inhibiting the harmful A1 phenotype while preserving neuroprotective functions. In-depth research targeting the cGAS/STING pathway may provide novel insights for simultaneously intervening in neuroinflammation and glial scar formation.

This study elucidates that HDAC7 drives astrocyte transformation toward the neurotoxic A1 phenotype via the IRF3/cGAS/STING pathway, revealing the dual regulatory mechanism of HDAC7 in neuroinflammation involving simultaneous activation in IRF3/cGAS/STING pathways. The anti-inflammatory effect of HDAC7 knockout provides novel therapeutic strategies for inflammation-related brain diseases such as neurodegenerative disorders and stroke; targeting HDAC7 or its downstream pathways holds promise as a precision medicine approach for intervening in central nervous system inflammation.

Data availability statement

The original contributions presented in this study are included in this article/Supplementary material, further inquiries can be directed to the corresponding authors.

Ethics statement

The animal studies were approved by Ethics Committee of Xinxiang Medical University. The studies were conducted in accordance with the local legislation and institutional requirements. Written informed consent was obtained from the owners for the participation of their animals in this study.

Author contributions

R-zY: Formal analysis, Writing – original draft, Methodology. XG: Data curation, Validation, Writing – review & editing. WL: Supervision, Resources, Writing – review & editing. CL: Formal analysis, Funding acquisition, Data curation, Writing – review & editing. LS: Investigation, Writing – review & editing, Writing – original draft, Conceptualization, Funding acquisition, Project administration.

Funding

The authors declare financial support was received for the research and/or publication of this article. This work was supported by the Natural Science Foundation of Henan Province (252300421392), Natural Science Foundation of Henan Province (232300420019), the Open Program of Henan Key Laboratory of Biological Psychiatry (ZDSYS2020004), and The College Students' Innovation and Entrepreneurship Training Programs of Henan Province (202410472003, 202510472014).

Conflict of interest

The authors declare that the research was conducted in the absence of any commercial or financial relationships that could be construed as a potential conflict of interest.

Generative AI statement

The authors declare that no Generative AI was used in the creation of this manuscript.

Any alternative text (alt text) provided alongside figures in this article has been generated by Frontiers with the support of artificial intelligence and reasonable efforts have been made to ensure accuracy, including review by the authors wherever possible. If you identify any issues, please contact us.

Publisher's note

All claims expressed in this article are solely those of the authors and do not necessarily represent those of their affiliated organizations, or those of the publisher, the editors and the reviewers. Any product that may be evaluated in this article, or claim that may be made by its manufacturer, is not guaranteed or endorsed by the publisher.

Supplementary material

The Supplementary Material for this article can be found online at: https://www.frontiersin.org/articles/10.3389/fncel.2025. 1683595/full#supplementary-material

References

- Balka, K. R., Louis, C., Saunders, T. L., Smith, A. M., Calleja, D. J., D'Silva, D. B., et al. (2020). TBK1 and IKK ϵ act redundantly to mediate STING-Induced NF- κ B responses in myeloid cells. *Cell Rep.* 31:107492. doi: 10.1016/j.celrep.2020.03.056
- Batiuk, M. Y., Martirosyan, A., Wahis, J., de Vin, F., Marneffe, C., Kusserow, C., et al. (2020). Identification of region-specific astrocyte subtypes at single cell resolution. *Nat. Commun.* 11:1220. doi: 10.1038/s41467-019-14198-8
- Beurel, E. (2011). HDAC6 regulates LPS-tolerance in astrocytes. PLoS One 6:e25804. doi: 10.1371/journal.pone.0025804
- Bignami, A., Eng, L. F., Dahl, D., and Uyeda, C. T. (1972). Localization of the glial fibrillary acidic protein in astrocytes by immunofluorescence. *Brain Res.* 43, 429–435. doi: 10.1016/0006-8993(72)90398-8
- Cai, L., Zeng, R., Huang, Q., Liu, X., Cao, Z., and Guo, Q. (2022). Paeonol inhibits chronic constriction injury-induced astrocytic activation and neuroinflammation in rats via the HDAC/miR-15a pathway. *Drug Dev. Res.* 83, 1758–1765. doi: 10.1002/ddr. 21993
- Cameron, E. G., Nahmou, M., Toth, A. B., Heo, L., Tanasa, B., Dalal, R., et al. (2024). A molecular switch for neuroprotective astrocyte reactivity. *Nature* 626, 574–582. doi: 10.1038/s41586-023-06935-3
- Decout, A., Katz, J. D., Venkatraman, S., and Ablasser, A. (2021). The cGAS–STING pathway as a therapeutic target in inflammatory diseases. *Nat. Rev. Immunol.* 21, 548–569. doi: 10.1038/s41577-021-00524-z
- Dräger, N. M., Sattler, S. M., Huang, C. T., Teter, O. M., Leng, K., Hashemi, S. H., et al. (2022). A CRISPRi/a platform in human iPSC-derived microglia uncovers regulators of disease states. *Nat. Neurosci.* 25, 1149–1162. doi: 10.1038/s41593-022-01131-4
- Escartin, C., Galea, E., Lakatos, A., O'Callaghan, J. P., Petzold, G. C., Serrano-Pozo, A., et al. (2021). Reactive astrocyte nomenclature, definitions, and future directions. *Nat. Neurosci.* 24, 312–325. doi: 10.1038/s41593-020-00783-4
- Fang, Y., Ding, X., Zhang, Y., Cai, L., Ge, Y., Ma, K., et al. (2022). Fluoxetine inhibited the activation of A1 reactive astrocyte in a mouse model of major depressive disorder through astrocytic 5-HT(2B)R/beta-arrestin2 pathway. *J. Neuroinflamm*. 19:23. doi: 10.1186/s12974-022-02389-y
- Glauben, R., Sonnenberg, E., Zeitz, M., and Siegmund, B. (2009). HDAC inhibitors in models of inflammation-related tumorigenesis. *Cancer Lett.* 280, 154–159. doi: 10.1016/j.canlet.2008.11.019
- Govindarajulu, M., Ramesh, S., Beasley, M., Lynn, G., Wallace, C., Labeau, S., et al. (2023). Role of cGAS-Sting signaling in Alzheimer's disease. *Int. J. Mol. Sci.* 24:8151. doi: 10.3390/iims24098151
- Guo, Q., Gobbo, D., Zhao, N., Zhang, H., Awuku, N. O., Liu, Q., et al. (2024). Adenosine triggers early astrocyte reactivity that provokes microglial responses and drives the pathogenesis of sepsis-associated encephalopathy in mice. *Nat. Commun.* 15:6340. doi: 10.1038/s41467-024-50466-y
- Hanslik, K. L., Marino, K. M., and Ulland, T. K. (2021). Modulation of glial function in health, aging, and neurodegenerative disease. *Front. Cell. Neurosci.* 15:718324. doi: 10.3389/fncel.2021.718324
- Hibbs, J. B. Jr., Taintor, R. R., Vavrin, Z., and Rachlin, E. M. (1988). Nitric oxide: A cytotoxic activated macrophage effector molecule. *Biochem. Biophys. Res. Commun.* 157, 87–94. doi: 10.1016/s0006-291x(88)80015-9
- Hinkle, J. T., Dawson, V. L., and Dawson, T. M. (2019). The A1 astrocyte paradigm: New avenues for pharmacological intervention in neurodegeneration. *Movement Disord.* 34, 959–969. doi: 10.1002/mds.27718
- Hinkle, J. T., Patel, J., Panicker, N., Karuppagounder, S. S., Biswas, D., Belingon, B., et al. (2022). STING mediates neurodegeneration and neuroinflammation in nigrostriatal α-synucleinopathy. *Proc. Natl. Acad. Sci. U. S. A.* 119:e2118819119. doi: 10.1073/pnas
- Hockfield, S. R. D. M., and McKay, R. D. (1985). Identification of major cell classes in the developing mammalian nervous system. *J. Neurosci.* 5, 3310–3328. doi: 10.1523/JNEUROSCI.05-12-03310.1985
- Jiao, P., Fan, W., Ma, X., Lin, R., Zhao, Y., Li, Y., et al. (2023). SARS-CoV-2 nonstructural protein 6 triggers endoplasmic reticulum stress-induced autophagy to degrade STING1. *Autophagy* 19, 3113–3131. doi: 10.1080/15548627.2023.2238579
- Jung, B. K., Park, Y., Yoon, B., Bae, J. S., Han, S. W., Heo, J. E., et al. (2023). Reduced secretion of LCN2 (lipocalin 2) from reactive astrocytes through autophagic and proteasomal regulation alleviates inflammatory stress and neuronal damage. *Autophagy* 19, 2296–2317. doi: 10.1080/15548627.2023.2180202
- Kadier, K., Niu, T., Ding, B., Chen, B., Qi, X., Chen, D., et al. (2024). PROTAC-Mediated HDAC7 protein degradation unveils its deacetylase-independent proinflammatory function in macrophages. *Adv. Sci.* 11:e2309459. doi: 10.1002/advs. 202309459
- Kim, H., Leng, K., Park, J., Sorets, A. G., Kim, S., Shostak, A., et al. (2022). Reactive astrocytes transduce inflammation in a blood-brain barrier model through a TNF-STAT3 signaling axis and secretion of alpha 1-antichymotrypsin. *Nat. Commun.* 13:6581. doi: 10.1038/s41467-022-34412-4

- Kjeldsen, L., Bainton, D. F., Sengelov, H., and Borregaard, N. (1994). Identification of neutrophil gelatinase-associated lipocalin as a novel matrix protein of specific granules in human neutrophils. *Blood* 83, 799–807. doi: 10.1182/blood.V83.3. 799.799
- Kujubu, D. A., Fletcher, B. S., Varnum, B. C., Lim, R. W., and Herschman, H. R. (1991). TIS10, a phorbol ester tumor promoter-inducible mRNA from Swiss 3T3 cells, encodes a novel prostaglandin synthase/cyclooxygenase homologue. *J. Biol. Chem.* 266, 12866–12872. doi: 10.1016/S0021-9258(18)98774-0
- Liang, P., Zhang, X., Zhang, Y., Wu, Y., Song, Y., Wang, X., et al. (2023). Neurotoxic A1 astrocytes promote neuronal ferroptosis via CXCL10/CXCR3 axis in epilepsy. *Free Radical Biol. Med.* 195, 329–342. doi: 10.1016/j.freeradbiomed.2023.01.002
- Liddelow, S. A., Guttenplan, K. A., Clarke, L. E., Bennett, F. C., Bohlen, C. J., Schirmer, L., et al. (2017). Neurotoxic reactive astrocytes are induced by activated microglia. *Nature* 541, 481–487. doi: 10.1038/nature21029
- Losarwar, S., Pancholi, B., Babu, R., and Garabadu, D. (2025). Mitochondria-dependent innate immunity: A potential therapeutic target in Flavivirus infection. *Int. Immunopharmacol.* 154:114551. doi: 10.1016/j.intimp.2025.114551
- Lu, Y., Zhao, Y., Gao, C., Suresh, S., Men, J., Sawyers, A., et al. (2024). HDAC5 enhances IRF3 activation and is targeted for degradation by protein C6 from orthopoxviruses including Monkeypox virus and Variola virus. *Cell Rep.* 43:113788. doi: 10.1016/j.celrep.2024.113788
- Lun, J., Li, Y., Gao, X., Gong, Z., Chen, X., Zou, J., et al. (2023). Kynurenic acid blunts A1 astrocyte activation against neurodegeneration in HIV-associated neurocognitive disorders. *J. Neuroinflamm.* 20:87. doi: 10.1186/s12974-023-02771-4
- Manengu, C., Zhu, C. H., Zhang, G. D., Tian, M. M., Lan, X. B., Tao, L. J., et al. (2024). HDAC inhibitors as a potential therapy for chemotherapy-induced neuropathic pain. *Inflammopharmacology* 32, 2153–2175. doi: 10.1007/s10787-024-01488-x
- Moncada, S. R. M. J., Palmer, R. M. L., and Higgs, E. (1991). Nitric oxide: Physiology, pathophysiology, and pharmacology. *Pharmacol. Rev.* 43, 109–142. doi: 10.1016/S0031-6997(25)06663-3
- Newman, L. E., Weiser Novak, S., Rojas, G. R., Tadepalle, N., Schiavon, C. R., Grotjahn, D. A., et al. (2024). Mitochondrial DNA replication stress triggers a proinflammatory endosomal pathway of nucleoid disposal. *Nat. Cell Biol.* 26, 194–206. doi: 10.1038/s41556-023-01343-1
- Oduro, P. K., Zheng, X., Wei, J., Yang, Y., Wang, Y., Zhang, H., et al. (2022). The cGAS-STING signaling in cardiovascular and metabolic diseases: Future novel target option for pharmacotherapy. *Acta Pharm Sin B* 12, 50–75. doi: 10.1016/j.apsb.2021.05.
- Paul, B. D., Snyder, S. H., and Bohr, V. A. (2021). Signaling by cGAS-STING in neurodegeneration, neuroinflammation, and aging. *Trends Neurosci.* 44, 83–96. doi: 10.1016/j.tins.2020.10.008
- Ramnath, D., Das Gupta, K., Wang, Y., Abrol, R., Curson, J. E. B., Lim, J., et al. (2022). The histone deacetylase Hdac7 supports LPS-inducible glycolysis and II-1β production in murine macrophages via distinct mechanisms. *J. Leukocyte Biol.* 111, 327–336. doi: 10.1002/jlb.2mr1021-260r
- Rosenblum, L. T., Shamamandri-Markandaiah, S., Ghosh, B., Foran, E., Lepore, A. C., Pasinelli, P., et al. (2017). Mutation of the caspase-3 cleavage site in the astroglial glutamate transporter EAAT2 delays disease progression and extends lifespan in the SOD1-G93A mouse model of ALS. *Exp. Neurol.* 292, 145–153. doi: 10.1016/j.expneurol.2017.03.014
- Segarra, M., Aburto, M. R., Hefendehl, J., and Acker-Palmer, A. (2019). Neurovascular interactions in the nervous system. *Ann. Rev. Cell Dev. Biol.* 35, 615–635. doi: 10.1146/annurev-cellbio-100818-125142
- Sethuraman, R., Lee, T. L., and Tachibana, S. (2009). D-serine regulation: A possible therapeutic approach for central nervous diseases and chronic pain. *Mini Rev. Med. Chem.* 9, 813–819. doi: 10.2174/138955709788452630
- Shakespear, M. R., Halili, M. A., Irvine, K. M., Fairlie, D. P., and Sweet, M. J. (2011). Histone deacetylases as regulators of inflammation and immunity. *Trends Immunol.* 32, 335–343. doi: 10.1016/j.it.2011.04.001
- Sun, M., Song, Y., Hu, X., Zhang, Z., Tan, R., Cai, Z., et al. (2025). Leptin reduces LPS-induced A1 reactive astrocyte activation and inflammation via inhibiting p38-MAPK signaling pathway. *Glia* 73, 25–37. doi: 10.1002/glia.24611
- Vecino, E., Rodriguez, F. D., Ruzafa, N., Pereiro, X., and Sharma, S. C. (2016). Glia–neuron interactions in the mammalian retina. *Prog. Retinal Eye Res.* 51, 1–40. doi: 10.1016/j.preteyeres.2015.06.003
- Villarreal, A., Vidos, C., Monteverde Busso, M., Cieri, M. B., and Ramos, A. J. (2021). Pathological neuroinflammatory conversion of reactive astrocytes is induced by microglia and involves chromatin remodeling. *Front. Pharmacol.* 12:689346. doi: 10.3389/fphar.2021.689346
- Wang, H. K., Su, Y. T., Ho, Y. C., Lee, Y. K., Chu, T. H., Chen, K. T., et al. (2023). HDAC1 is involved in neuroinflammation and blood-brain barrier damage in stroke pathogenesis. *J. Inflamm. Res.* 16, 4103–4116. doi: 10.2147/jir.S416239

- Wang, S., Pan, Y., Zhang, C., Zhao, Y., Wang, H., Ma, H., et al. (2024). Transcriptome analysis reveals dynamic microglial-induced A1 astrocyte reactivity via C3/C3aR/NF- κ B signaling after ischemic stroke. *Mol. Neurobiol.* 61, 10246–10270. doi: 10.1007/s12035-024-04210-8
- Wen, L., Bi, D., and Shen, Y. (2024). Complement-mediated synapse loss in Alzheimer's disease: Mechanisms and involvement of risk factors. *Trends Neurosci.* 47, 135–149. doi: 10.1016/j.tins.2023.11.010
- West, A. P., Khoury-Hanold, W., Staron, M., Tal, M. C., Pineda, C. M., Lang, S. M., et al. (2015). Mitochondrial DNA stress primes the antiviral innate immune response. *Nature* 520, 553–557. doi: 10.1038/nature14156
- Willis, E. F., MacDonald, K. P. A., Nguyen, Q. H., Garrido, A. L., Gillespie, E. R., Harley, S. B. R., et al. (2020). Repopulating microglia promote brain repair in an IL-6-Dependent manner. *Cell* 180, 833–846 e16. doi: 10.1016/j.cell.2020.02.013.
- Wu, Q., Leng, X., Zhang, Q., Zhu, Y. Z., Zhou, R., Liu, Y., et al. (2024). IRF3 activates RB to authorize cGAS-STING–induced senescence and mitigate liver fibrosis. *Sci. Adv.* 10:eadj2102. doi: 10.1126/sciadv.adj2102
- Xia, Z., Luo, T., Liu, H. M., Wang, F., Xia, Z. Y., Irwin, M. G., et al. (2010). Larginine enhances nitrative stress and exacerbates tumor necrosis factor- α toxicity to human endothelial cells in culture: Prevention by propofol. *J. Cardiovasc. Pharmacol.* 55, 358–367. doi: 10.1097/FJC.0b013e3181d265a3
- Xiong, X.-Y., Tang, Y., and Yang, Q.-W. (2022). Metabolic changes favor the activity and heterogeneity of reactive astrocytes. *Trends Endocrinol. Metab.* 33, 390–400. doi: 10.1016/j.tem.2022.03.001
- Yao, F., Jin, Z., Zheng, Z., Lv, X., Ren, L., Yang, J., et al. (2022). HDAC11 promotes both NLRP3/caspase-1/GSDMD and caspase-3/GSDME pathways causing pyroptosis via ERG in vascular endothelial cells. *Cell Death Discovery* 8:112. doi: 10.1038/s41420-022-00906-9

- Ye, J., Zhong, S., Deng, Y., Yao, X., Liu, Q., Wang, J. Z., et al. (2022). HDAC7 activates IKK/NF-kappaB signaling to regulate astrocyte-mediated inflammation. *Mol. Neurobiol.* 59, 6141–6157. doi: 10.1007/s12035-022-02965-6
- Ye, J., Zhong, S., Wan, H., Guo, X., Yao, X., Liu, Q., et al. (2025). Upregulated astrocyte HDAC7 induces Alzheimer-like tau pathologies via deacetylating transcription factor-EB and inhibiting lysosome biogenesis. *Mol. Neurodegener.* 20:5. doi: 10.1186/s13024-025-00796-2
- Yun, S. P., Kam, T. I., Panicker, N., Kim, S., Oh, Y., Park, J. S., et al. (2018). Block of A1 astrocyte conversion by microglia is neuroprotective in models of Parkinson's disease. *Nat. Med.* 24, 931–938. doi: 10.1038/s41591-018-0051-5
- Zhang, D., Liu, C., Li, H., and Jiao, J. (2020). Deficiency of STING signaling in embryonic cerebral cortex leads to neurogenic abnormalities and autistic-like behaviors. *Adv. Sci.* 7:2002117. doi: 10.1002/advs.202002117
- Zhang, J., Rong, P., Zhang, L., He, H., Zhou, T., Fan, Y., et al. (2021). IL4-driven microglia modulate stress resilience through BDNF-dependent neurogenesis. *Sci. Adv.* 7:eabb9888. doi: 10.1126/sciadv.abb9888
- Zhang, Y., Chen, Q., Chen, D., Zhao, W., Wang, H., Yang, M., et al. (2021). SerpinA3N attenuates ischemic stroke injury by reducing apoptosis and neuroinflammation. *CNS Neurosci. Therapeut.* 28, 566–579. doi: 10.1111/cns.
- Zhang, Z., Li, D., Xu, L., and Li, H. P. (2019). Sirt1 improves functional recovery by regulating autophagy of astrocyte and neuron after brain injury. *Brain Res. Bull.* 150, 42–49. doi: 10.1016/j.brainresbull.2019.05.005
- Zhang, Z., Zhang, X., Wu, X., Zhang, Y., Lu, J., and Li, D. (2022). Sirt1 attenuates astrocyte activation via modulating Dnajb1 and chaperone-mediated autophagy after closed head injury. *Cereb. Cortex* 32, 5191–5205. doi: 10.1093/cercor/bhac007